Case Studies in Thermal Engineering 52 (2023) 103752

Contents lists available at ScienceDirect

Case Studies in Thermal Engineering

journal homepage: www.elsevier.com/locate/csite

The effect of a reversed circular jet impingement on A bifacial module PVT collector energy performance

Muhammad Amir Aziat Bin Ishak [a], Adnan Ibrahim [a,*], Mohd Faizal Fauzan [a], Ahmad Fazlizan [a], Win Eng Ewe [b], Hussein A. Kazem [c]

[a] *Solar Energy Research Institute, Universiti Kebangsaan Malaysia, 43600, Bangi, Selangor, Malaysia*
[b] *Energy Systems Research Unit, Mechanical and Aerospace Engineering, University of Strathclyde, Glasgow, G1 1XJ, Scotland, United Kingdom*
[c] *Faculty of Engineering, Sohar University, PO Box 44, Sohar, PCI 311, Oman*

A R T I C L E I N F O

Handling Editor: Huihe Qiu

Keywords:
Jet impingement
Photovoltaic thermal (PVT)
Bifacial module
Solar collector
Cooling method

A B S T R A C T

Photovoltaic thermal (PVT) technologies have a significant downside in addition to their numerous advantages. PVT technologies are constrained by the fact that its photovoltaic module gains heat due to exposure to solar irradiance, which reduces the photovoltaic efficiency. Jet impingement is one of the most effective methods to cool a photovoltaic module. An indoor experiment using a solar simulator was conducted on a bifacial PVT solar collector cooled by a reversed circular flow jet impingement (RCFJI) to evaluate the energy performance of the PVT collector. The study was conducted under a constant solar irradiance of 900W/m^2 and flowrate (mass) ranging from 0.01 to 0.14 kg/s. Three bifacial modules with 0.22, 0.33, and 0.66 packing factors were mounted 25 mm above the RCFJI for cooling. The 0.66 packing factor module recorded the highest photovoltaic efficiency of 10.91 % at 0.14 kg/s flowrate (mass). Meanwhile, the 0.22 and 0.33 packing factors recorded a photovoltaic efficiency of 4.50 % and 6.45 %, respectively. The highest thermal efficiency recorded under the same operating condition was 61.43 %, using a 0.66 packing factor. Overall, the highest combined photovoltaic thermal (PVT) efficiency for 0.22, 0.33, and 0.66 was 56.62 %, 61.88 %, and 72.35 %, respectively.

1. Introduction

Photovoltaic thermal (PVT) technologies have the ability to generate both electrical and thermal energy simultaneously [1]. Analyst has predicted that its durability could last up to 30 years [2]. PVT technologies have the potential to replace conventional energy production [3]. PVT technologies rely on the photovoltaic (PV) module, which is an integral part of the system [4]. There are two common types of photovoltaic modules: mono-facial and bifacial modules. A mono-facial module can only generate electricity by absorbing sunlight from the front side of the module, whereas a bifacial module can generate electricity from both front and rear sides of the module surface [5]. The surface area exposed to solar irradiance is maximized in bifacial module [6].

Despite the numerous benefits offered by PVT technologies, it also possesses a notable drawback. PVT technologies are subjected to a constraint where the photovoltaic module gains heat due to exposure to the solar irradiance, which consequently leads to a reduction in the photovoltaic efficiency [7]. Thus, to improve the performance of a PVT collector, a cooling system is necessary [8,9]. Cooling methods for bifacial modules are limited since both sides of the bifacial modules need to be exposed to the sunlight [10]. One of the

* Corresponding author.
E-mail address: iadnan@ukm.edu.my (A. Ibrahim).

https://doi.org/10.1016/j.csite.2023.103752
Received 25 January 2023; Received in revised form 6 November 2023; Accepted 9 November 2023
Available online 11 November 2023

effective methods to cool down a bifacial module is introducing a jet impingement method [11]. The impinging effect increases the heat transfer rate inside the PVT collector, which can improve the PV module efficiency. This study conducted an indoor experiment to analyze the performance of three bifacial modules with different packing factors cooled by a reversed circular flow jet impingement (RCFJI). This study addresses a research gap in the solar collector cooling mechanism involving the jet impingement method. Additionally, it contributes to proposing a technique to improve the performance and efficiency of a bifacial PVT collector. The impinging effects on the PV module through the jet impingement method result in a significant heat transfer rate. Nonetheless, as stated by Ewe et al., 2021, research on the utilization of jet impingement method in bifacial module applications is limited. Extensive studies are necessary to effectively explore the potential of jet impingement method [12].

The reversed circular flow jet impingement (RCFJI) bifacial PVT solar collector comprises three primary components: The PVT solar collector, the bifacial module, and the jet plate. PVT technologies rely on the photovoltaic module, which is an integral part of the system [4]. Three bifacial modules with different packing factors of 0.22, 0.33, and 0.66 were utilized in this study, as depicted in Fig. 1. Packing factor refers to the proportion of the photovoltaic module's surface area that is occupied by the solar cell [13]. The RCFJI was tested on three bifacial modules with different packing factors to observe the performance consistency of the RCFJI on different bifacial modules. The bifacial modules utilized in this study are custom-made photovoltaic modules ordered by The Solar Energy Research Institute (SERI), Universiti Kebangsaan Malaysia. The bifacial module is made from Mono-crystalline silicon cells, and its surface is constructed from transparent tempered glass, which permits the penetration of sunlight through the bifacial module. The bifacial module is mounted 25 mm above a stainless-steel jet plate with mirror polished finishing to allow the sunlight that passes through the bifacial module to be reflected back on to the rear side of the bifacial modules. Thus, more electrical energy can be produced as both sides of the module can generate electricity. Table 1 provides the details for the bifacial modules.

The bifacial PVT solar collector measures 770 mm length x 820 mm width x 194 mm height. The RCFJI cup measures 40 mm in diameter and 20 mm in depth is attached to the back of the jet plate with 36 holes, each 3 mm in diameter with 126 mm spanwise and 113.4 mm streamwise, as illustrated in Fig. 2. The jet plate has a highly reflective surface, n_r of 0.7 to reflect the sunlight onto the rear side of the bifacial module. The jet plate is then mounted 25 mm below the bifacial module. Air is distributed through a 6 mm polyurethane tube connected to the RCFJI inlet. The air enters the RCFJI cup to create a circular airflow motion before leaving the 3 mm jet plate holes at high velocity, causing an impinging impact on the bifacial module.

2. Experiment setup

An indoor experiment was conducted at SERI, Universiti Kebangsaan Malaysia, to analyze the energy performance of a bifacial PVT solar collector cooled by a reversed circular jet impingement, as shown in Fig. 3. A solar simulator with 32 tungsten halogen lights (500 W each) was used. 14 K-type thermocouples connected to an AT4824 Data logger were calibrated before placing them around the RCFJI bifacial PVT collector. The experiment procedure was conducted in accordance with a methodology devised based on prior research [10,14].

The experiment used forced convection from a high-velocity air compressor. An anemometer sets the compressor's air inlet flowrate to a constant flow (mass). The flowrate (mass) ranges from 0.01 to 0.14 kg/s, and the solar irradiation was set to $900W/m^2$. The solar irradiance was adjusted to $900W/m^2$ and monitored using a pyranometer. Three bifacial modules with 0.66, 0.33, and 0.22 packing factors were tested to analyze the PVT collector's performance cooled by a reversed circular jet impingement (RCFJI). The data logger recorded the RCFJI temperature every 1 s for 30 min. After 25–30 min, the system attained a steady state with no temperature changes. An MP-11 I–V tracer connected to the bifacial module was used to record the current, voltage, and power of the bifacial module at the steady state. It was later imported to Microsoft Excel to be analyzed. The collector was left to cool down for 2 h before repeating the same procedure using a different packing factor bifacial module.

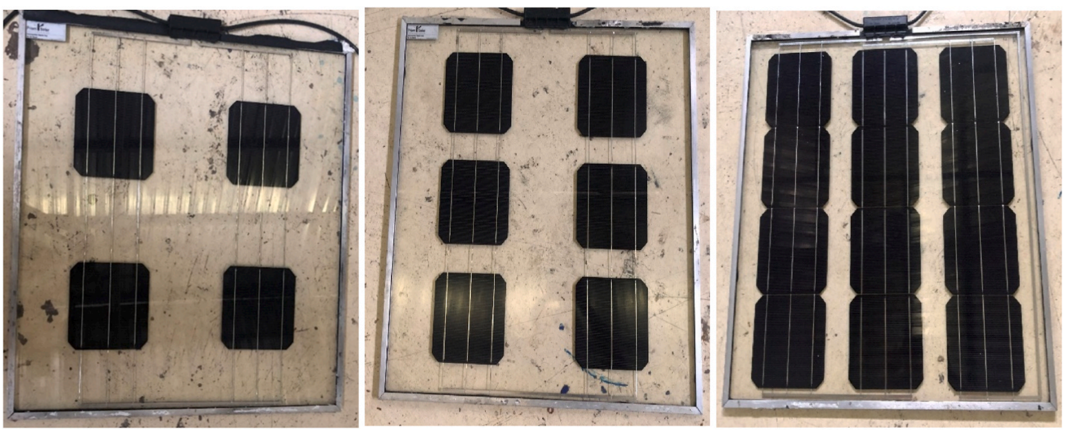

Fig. 1. Bifacial module from left 0.22, 0.33, and 0.66 packing factor.

Table 1
Bifacial module details.

Parameters	Value		
Packing factor	0.66	0.33	0.22
Rated maximum power (P_{max})	60w	40w	20w
Voltage at maximum power (V_{MP})	17.14	12	8.33
Current at maximum power (I_{MP})	3.5	3.33	2.4
Open circuit voltage (V_{OC})	22.1	17.8	14.5
Short circuit current (I_{SC})	3.71	3.35	2.75

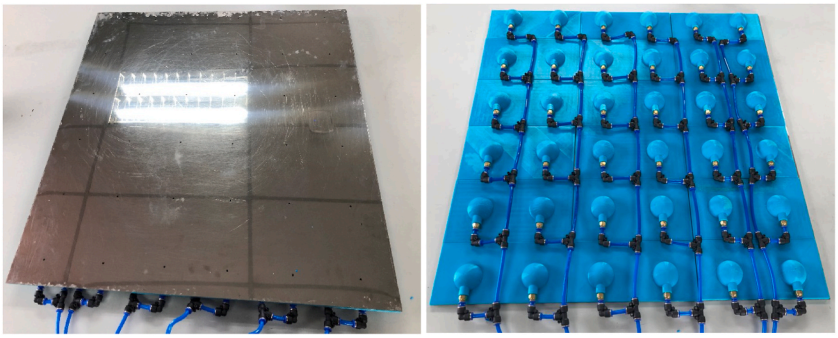

Fig. 2. Top view (left) and bottom view (right) of the RCFJI attached to the back of a jet plate.

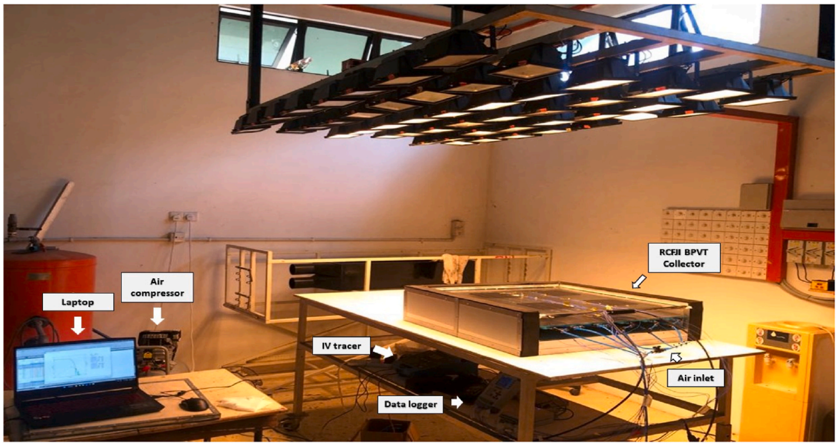

Fig. 3. Experiment setup.

Table 2
Indices and values.

Parameter	Value
Flowrate (mass), $\dot{m}$	0.1–0.14 kg/s
Width of collector, W	684 mm
Length of collector, L	705 mm
Duct Depth, d	25 mm
Solar irradiance, I	900 W/m^2
Area of collector, Ac	0.48 m^2
Absorptivity of PV cell, α_{pv}	0.91
Packing factor, P	0.22, 0.33, 0.66
Transmittance of Lamination, τ_1	0.85
Reflectivity of the jet plate, n_r	0.7
Electrical efficiency at reference condition, n_{ref}	0.16
Temperature Coefficient, β	0.0045 K^{-1}
Temperature at reference condition, T_{ref}	303.15 K

3. Energy analysis

The energy efficiency of the three bifacial modules cooled by a reversed circular jet impingement was analyzed. Table 2 lists all of the indices and values from the energy analysis.

3.1. Photovoltaic efficiency

Photovoltaic efficiency is determined by using:

$$\eta_{Photovoltaic} = \frac{Pmax}{(I\ x\ Ac)} \tag{1}$$

An I–V tracer is used to determine *Pmax*, which is stated as [15]:

$$P_{max} = IA_c\alpha_{pv}P(\eta_{pvfront}) + IA_c\tau_i(1-P)n_r\alpha_{pv}P(\eta_{pvrear}) \tag{2}$$

The bifacial cell's efficiency is denoted by the formula [15]:

$$\eta_{pvfront} = \eta_{pvrear} = \eta_{ref}\left[1 - B\left(T_{pv} - T_{ref}\right)\right] \tag{3}$$

3.2. Thermal efficiency

Thermal efficiency, $\eta_{thermal}$, is expressed as [12]:

$$\eta_{Thermal} = \frac{Qu}{(I\ x\ Ac)} \tag{4}$$

When expressing useful heat gain, *Qu*:

$$Qu = \dot{m}C_p(T_o - T_i) \tag{5}$$

The air's specific heat capacity, *Cp*, is represented as [16]:

$$C_p = 1.0057 + 0.000066(T - 300) \tag{6}$$

3.3. Combined photovoltaic thermal efficiency

The combined photovoltaic thermal efficiency is calculated using the following:

$$\eta_{photovoltaic\ thermal} = \eta_{Photovoltaic} \times \eta_{Thermal} \tag{7}$$

3.4. Compressor pumping power

The pumping power for the RCFJI was evaluated to analyze the power consumed against the photovoltaic and thermal power generated. Based on the equation below, the RCFJI pumping power for all the bifacial modules is the same. The compressor power, Cpp, is determined as follows [15,17]:

$$C_{pp} = \frac{\dot{m} \times \Delta P}{\rho} \tag{8}$$

The pressure drops, ΔP, is presented as:

$$\Delta P = \Delta P1 + \Delta P2 \tag{9}$$

The pressure drop for the RCFJI, ΔP1, and the upper channel is defined as:

$$\Delta P1 = \frac{2f_1 \times LG_1{}^2}{D_h \times \rho}, \Delta P2 = \frac{2f_1 \times LG_2{}^2}{D_h \times \rho} \tag{10}$$

The friction factor for the RCFJI cup, f_1, is presented as [15,17]:

$$f_1 = 0.085 \times \left(Re^{-0.25}\right) \tag{11}$$

And the friction factor for the upper channel is presented as [15,17]:

$$f_2 = 0.3475 \times \left(Re^{-0.5244}\right) \times \left[\left(\frac{X}{D_h}\right)^{0.4169}\right] \times \left[\left(\frac{Y}{D_h}\right)^{0.5321}\right] \times \left[\left(\frac{D_j}{D_h}\right)^{-1.4848}\right]$$

$$\times exp\left[-0.2210 \times \left(\ln\frac{D_j}{D_h}\right)^2\right] \tag{12}$$

The hydraulic diameter, D_h, is defined as:

$$D_h = \frac{4WD}{2(W + D)} \tag{13}$$

The air mass velocity distributed through the systems is defined as:

$$G_1 = G_2 = \frac{\dot{m}}{(W \times d)} \tag{14}$$

3.5. Uncertainty analysis

Uncertainty analysis was used to systematically measure approximation inaccuracies, measurement errors, and the data's accuracy. As stated in Table 3, uncertainty analysis was done on every measuring apparatus to determine the degree of uncertainty. The uncertainty level of the apparatus was less than 2 %. Hence, the experimental result could be considered reliable and accurate. Calculating the standard deviation, s, is expressed as [10]:

$$s = \sqrt{\frac{\sum_i^n (x_i - \overline{x})^2}{n-1}} \tag{15}$$

Where x_i, $\overline{x}$, and n represents the means of measurement, measurement results, and sets of measurement. The expression for the uncertainty, u, is as follows [10]:

$$u = \frac{s}{\sqrt{n}} \tag{16}$$

4. Results and discussions

4.1. Photovoltaic efficiency

The photovoltaic efficiency of the three distinct bifacial modules cooled by a reversed circular jet impingement (RCFJI) was examined, as per Fig. 4. The 0.66 packing factor temperature ranges between 44.3 and 55.2 °C while the 0.33 and 0.22 packing factor ranges between 41.2 and 51.8 °C and 39.1–49.3 °C. The photovoltaic efficiency for 0.66, 0.33, and 0.22 packing factors was 10.18–10.91 %, 6.12–6.45 %, and 4.27–4.50 %. The 0.66 packing factor module achieved the highest photovoltaic efficiency with a maximum photovoltaic efficiency of 10.91 %. With increasing flowrate (mass), a slight improvement can be seen in the photovoltaic efficiency. Increasing the flowrate (mass) enhances airflow and heat transfer in the collector, which helps to reduce the module temperature. It can be observed that the photovoltaic efficiency increases as the module temperature decreases. In addition, a higher packing factor module recorded a higher photovoltaic efficiency as it has more solar cells to generate electricity.

Fig. 5 presents the current, I, and power, P against voltage, V graph of the bifacial PVT collector at 900W/m^2 and 0.14 kg/s flowrate (mass). The highest I–V performances were achieved using a 0.66 packing factor with a current of 3.54A and voltage of 19.87V. The highest Pmax value achieved was 46.87W with a voltage of 3.54A using 0.66 packing factor. The Pmax recorded for 0.33, and 0.22 packing was 26.87W and 18.11W. From the observation, bifacial module with a higher packing factor generates more current and voltage compared to a lower packing factor module.

4.2. Thermal efficiency

From Fig. 6, the outlet temperature drops as the flowrate (mass) increases. The highest outlet temperature was achieved by a 0.66 packing factor with an outlet temperature of 35.13–43.93 °C, followed by 0.33 and 0.22 packing factors with 33.03–40.87 °C and 32.13–39.53 °C, respectively. The outlet temperature, T_{out}, inlet temperature, T_{in}, and temperature difference, ΔT, of the RCFJI on a bifacial module with different packing factors are presented in Table 4. The highest thermal efficiency recorded was 61.43 % using a 0.66 packing factor at 0.14 kg/s flowrate (mass). The lowest thermal efficiency achieved was 52.12 % at 0.14 kg/s using a 0.22 packing factor. Under the same conditions, the 0.33 packing factor achieved 55.43 % thermal efficiency. It was observed that higher packing factor modules result in a higher outlet temperature, as more bifacial cells covering the bifacial modules, and thus, more heat is gained. In addition, higher thermal efficiency was achieved using a higher packing factor module.

4.3. Power consumed against power generated

The compressor pumping power, Cpp, was assessed to examine the power consumed by the bifacial PVT collector in relation to the photovoltaic and thermal power generated. Based on the results, the highest photovoltaic and thermal efficiency is obtained at the

Table 3
Uncertainty of the measuring apparatus.

Equipment	Model	Parameters	Unit	Uncertainty (%)
I–V tracer	MP-11	Solar irradiance	W/m^2	±0.65 %
Data Logger	AT4824	Temperature	°C	±0.1 °C
Thermocouples	K-type	Temperature	°C	±0.1 °C
Pyranometer	TES132	Solar irradiance	W/m^2	±1.3 %
Anemometer	MT-4615	Air velocity	m/s	±1.45 %

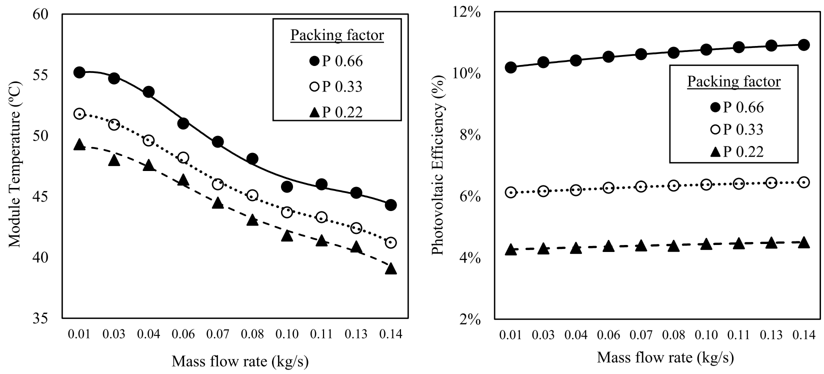

Fig. 4. Module temperature and photovoltaic efficiency at 900W/m^2 solar irradiance.

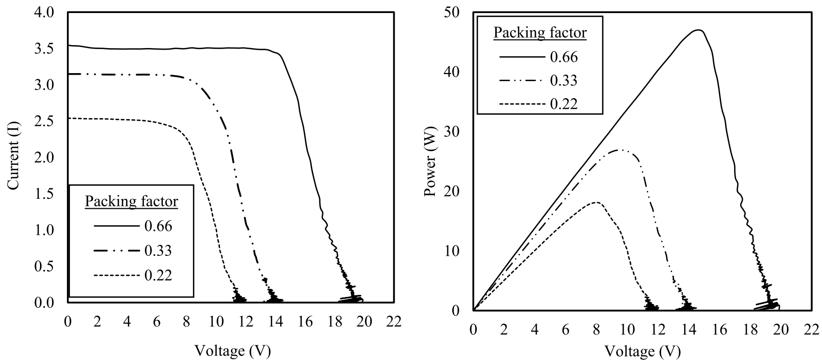

Fig. 5. I–V and P–V curves at 900W/m^2 solar irradiance.

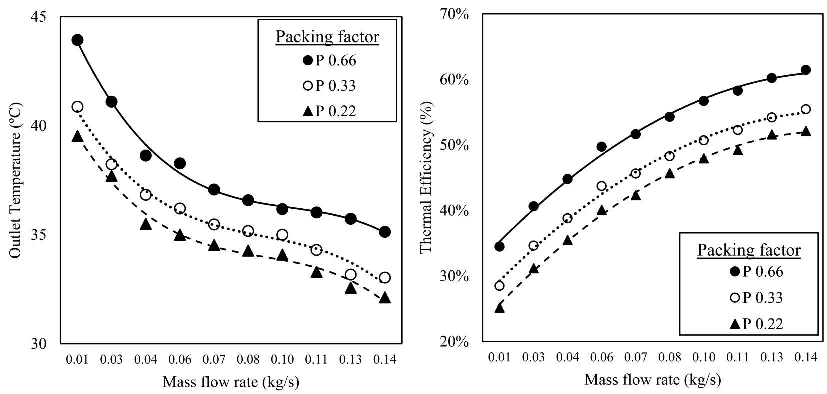

Fig. 6. Outlet temperature and thermal efficiency at 900W/m^2 solar irradiance.

highest mass flow rate. However, it must be emphasized that a higher mass flow rate increases the pumping power. Based on Fig. 7. The compressor pumping power exceeds the photovoltaic energy generated. This is due to the bifacial modules specification, which has a low-rated maximum power (Pmax), as presented in Table 1 is used. The maximum power that can be generated by the 0.66, 0.33, and 0.22 packing factors is 60W, 40W, and 20W only. Therefore, a bifacial module with a higher Pmax is needed to increase the photovoltaic energy production. Conversely, the thermal energy showed a higher energy generated compared to the compressor pumping power. Therefore, more useful heat and thermal energy could be utilized.

4.4. Combined photovoltaic thermal (PVT) efficiency

As shown in Fig. 8, a 0.66 bifacial module packing factor with a photovoltaic efficiency of 10.91 % and a thermal efficiency of

Table 4
Outlet temperature, inlet temperature, and temperature difference of RCFJI on different packing factor bifacial modules.

Mass flow rate	0.22			0.33			0.66		
	T_{out}	T_{in}	ΔT	T_{out}	T_{in}	ΔT	T_{out}	T_{in}	ΔT
0.01	39.53	31.81	7.72	40.87	32.13	8.74	43.93	33.35	10.58
0.03	37.70	32.92	4.78	38.23	32.92	5.31	41.10	34.87	6.23
0.04	35.50	31.87	3.63	36.83	32.86	3.97	38.63	34.05	4.58
0.06	35.00	31.92	3.08	36.20	32.85	3.35	38.27	34.46	3.81
0.07	34.53	31.93	2.60	35.47	32.67	2.80	37.07	33.90	3.17
0.08	34.27	31.93	2.34	35.17	32.70	2.47	36.58	33.80	2.78
0.10	34.09	31.99	2.10	35.00	32.78	2.22	36.17	33.68	2.49
0.11	33.30	31.41	1.89	34.30	32.29	2.01	36.02	33.78	2.24
0.13	32.57	30.81	1.76	33.17	31.32	1.85	35.73	33.68	2.05
0.14	32.13	30.53	1.60	33.03	31.33	1.70	35.13	33.24	1.89

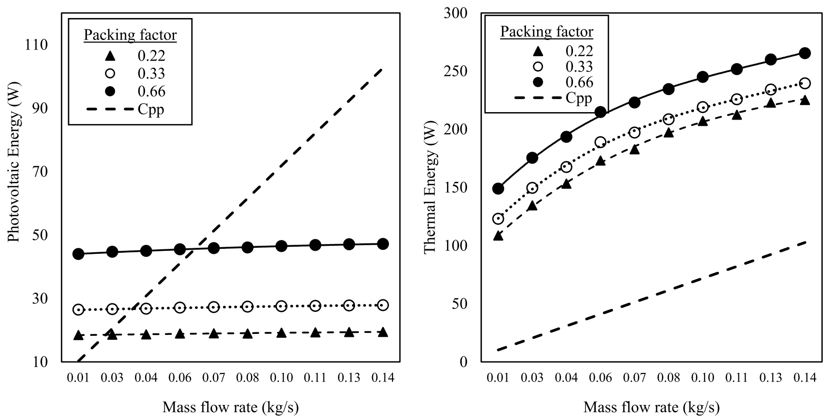

Fig. 7. Photovoltaic and thermal energy of RCFJI against pumping power.

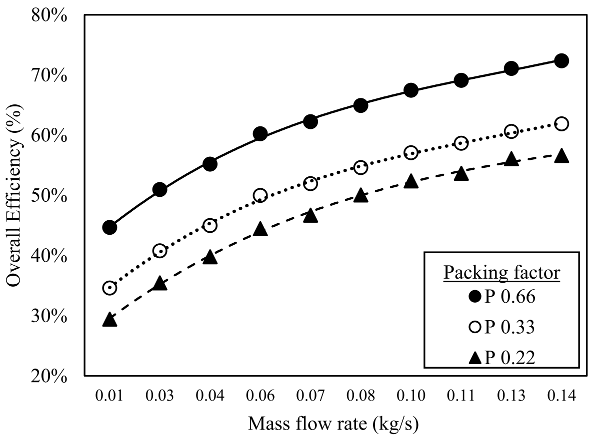

Fig. 8. Combined Photovoltaic thermal efficiency at 900W/m^2 solar irradiance.

61.43 % at 0.14 kg/s resulted in the highest combined PVT efficiency. In comparison to non-active cooling without the RCFJI, the bifacial PVT collector using a 0.66 packing factor module recorded a combined photovoltaic thermal efficiency of 61.78 % at 0.14 kg/s. A 10.57 % increment was observed when comparing the bifacial PVT solar collector with and without the RCFJI using the highest performance packing factor of 0.66. Meanwhile, under the same operating conditions, the 0.33 packing factor had a combined PVT efficiency of 61.88 %, while the 0.22 had the lowest at 56.62 %.

A comparison of the overall efficiency has been made between the bifacial PVT collector incorporating the RCFJI and without the RCFJI to observed the performance of the PVT collector, as shown in Fig. 9. Based on Fig. 9, it can be observed that the bifacial PVT collector incorporating the RCFJI has a significant increase in the overall efficiency compared to the bifacial PVT collector without the

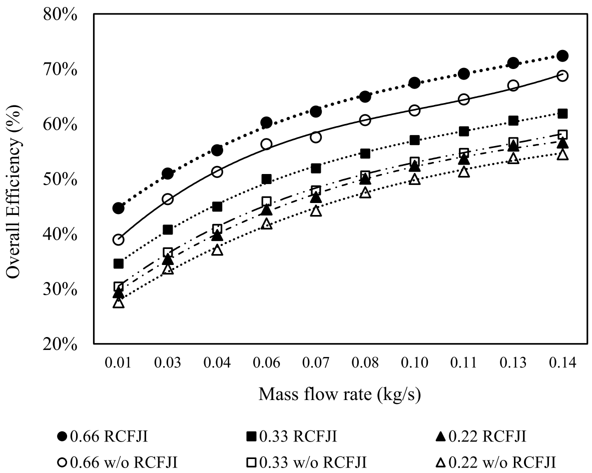

Fig. 9. Overall efficiency comparison between the bifacial PVT collector with RCFJI and without RCFJI.

RCFJI. From the findings, the 0.66 packing factor bifacial PVT collector achived an increasement in overall efficiency of 3.63%–5.74 % increase when compared to the PVT collector without the RCFJI. In addition, the 0.33 and 0.22 packing factor bifacial PVT collector recorded an increase of 3.83–4.17 % and 1.84–2.13 % in overall efficiency. Therefore, it can be concluded that the RCFJI contributes to enhancing the performance of the bifacial PVT collector.

5. Conclusion

An indoor experiment was conducted to analyze the energy performance of a reversed circular flow jet impingement (RCFJI) bifacial PVT collector. Three bifacial modules with different packing factors of 0.22, 0.33, and 0.66 were utilized for the experiment. The reversed circular flow jet impingement aids in cooling down the bifacial PVT collector, thereby enhancing its performance. According to the results obtained, it can be concluded that the bifacial module exhibiting a packing factor of 0.66 demonstrates the highest energy performance in comparison to the other two bifacial modules. The bifacial module with a packing factor of 0.66 exhibits a maximum photovoltaic efficiency of 10.91 % when subjected to a mass flow rate of 0.14 kg/s. In contrast, the modules with packing factors of 0.33 and 0.22 demonstrate efficiencies of 6.45 % and 4.50 %, respectively. The RCFJI technique improves the performance of the module by reducing the temperature of the bifacial module and helps recover the current and voltage loss. The maximum thermal efficiency was 61.43 % at 0.14 kg/s with a 0.66 packing factor. The lowest thermal efficiency was 52.12 %, with 0.22 packing under the same operating parameters. The combined PVT efficiency recorded by the 0.66, 0.33, and 0.22 packing factors was 72.35 %, 61.88 %, and the lowest, 56.62 %, respectively. Overall, the highest energy performance achieved was by using a 0.66 packing factor module with a maximum photovoltaic, thermal, and combined photovoltaic thermal efficiency of 10.91 %, 61.43 %, and 72.35 % at 0.14 kg/s mass flow rate. The RCFJI helps to reduce and cool down the module temperature of the bifacial module and the PVT collector. The impinging effect prevents the development of boundary layers on the bifacial module and increases PVT collector heat transfer. The RCFJI showed a consistent photovoltaic and thermal energy trend for all the bifacial modules tested.

Author statement

Muhammad Amir Aziat Bin Ishak devised the conceptual ideas, including writing, reviewing, designing the model, computational framework, data analysis, and draft preparation Mohd Faizal Fauzan, Ahmad Fazlizan, Win Eng Ewe, and Hussein A. Kazem verified the analytical methods and investigation. Adnan Ibrahim performed the visualization and funding acquisition and supervised the findings of this work.

Declaration of competing interest

The authors declare that they have no known competing financial interests or personal relationships that could have appeared to influence the work reported in this paper.

Data availability

Data will be made available on request.

Acknowledgment

The financial support by the Universiti Kebangsaan Malaysia through research funding of Dana Inovasi (INOVASI-2022-004) is gratefully acknowledged.

References

[1] Abdulsahib M. Bassam, Kamaruzzaman Sopian, Adnan Ibrahim, Mohd Faizal Fauzan, Anwer B. Al-Aasam, Ghaith Yahay Abusaibaa, Experimental analysis for the photovoltaic thermal collector (PVT) with nano PCM and micro-fins tube nanofluid, Case Stud. Therm. Eng. 41 (2022) (2023), 102579, https://doi.org/10.1016/j.csite.2022.102579.

[2] Adnan Ibrahim, Mohd Yusof Othman, Mohd Hafidz Ruslan, Sohif Mat, Kamaruzzaman Sopian, Recent advances in flat plate photovoltaic/thermal (PV/T) solar collectors, Renew. Sustain. Energy Rev. 15 (1) (2011) 352–365, https://doi.org/10.1016/j.rser.2010.09.024.

[3] Muhammad Aqil Afham Rahmat, Abd Ag Sufiyan, Yuanshen Hamid, Muhammad Amir Aziat Bin Lu, Shaikh Zishan Suheel Ishak, Fazlizan Ahmad, Ibrahim Adnan, "An analysis of renewable energy technology integration investments in Malaysia using HOMER pro", Sustain. Times 14 (20) (2022), https://doi.org/10.3390/su142013684.

[4] K. Sopian, K.S. Yigit, H.T. Liu, S. Kakaç, T.N. Veziroglu, Performance analysis of photovoltaic thermal air heaters, Energy Convers. Manag. 37 (11) (1996) 1657–1670, https://doi.org/10.1016/0196-8904(96)00010-6.

[5] Elumalai Vengadesan, Ramalingam Senthil, A review on recent developments in thermal performance enhancement methods of flat plate solar air collector, Renew. Sustain. Energy Rev. 134 (2020), 110315, https://doi.org/10.1016/j.rser.2020.110315. November 2019.

[6] Y. Chaibi, T. El Rha, R. Sim, O. Charro Gajate, T. Kousksou, Y. Zeraouli, "Air-based hybrid photovoltaic/thermal systems, A Rev. n-Allu e 295 (2021), https://doi.org/10.1016/j.jclepro.2021.126211.

[7] Mohammad Hemmat, Mohammad Hassan, Majid Valadkhani, Application of nanofluids and fluids in photovoltaic thermal system : an updated review, Sol. Energy 199 (2020) 796–818, https://doi.org/10.1016/j.solener.2020.01.015. February.

[8] Sébastien A. Brideau, Michael R. Collins, Development and validation of a hybrid PV/Thermal air based collector model with impinging jets, Sol. Energy 102 (2014) 234–246, https://doi.org/10.1016/j.solener.2014.01.022.

[9] Sébastien A. Brideau, Michael R. Collins, Experimental model validation of a hybrid PV/thermal air based collector with impinging jets, Energy Proc. 30 (2012) 44–54, https://doi.org/10.1016/j.egypro.2012.11.007.

[10] Poorya Ooshaksaraei, Kamaruzzaman Sopian, Saleem H. Zaidi, Rozli Zulkifli, Performance of four air-based photovoltaic thermal collectors configurations with bifacial solar cells, Renew. Energy 102 (2017) 279–293, https://doi.org/10.1016/j.renene.2016.10.043.

[11] Javad Mohammadpour, Fatemeh Salehi, Mohsen Sheikholeslami, Ann Lee, A computational study on nanofluid impingement jets in thermal management of photovoltaic panel, Renew. Energy 189 (2022) 970–982, https://doi.org/10.1016/j.renene.2022.03.069.

[12] Win Eng Ewe, Ahmad Fudholi, Kamaruzzaman Sopian, Nilofar Asim, Modeling of bifacial photovoltaic-thermal (PVT) air heater with jet plate, Int. J. Heat Technol. 39 (4) (Aug. 2021) 1117–1122, https://doi.org/10.18280/ijht.390409.

[13] Sourav Diwania, Sanjay Agrawal, Anwar S. Siddiqui, Sonveer Singh, Photovoltaic – thermal (PV/T) technology : a comprehensive review on applications and its advancement, Int. J. Energy Environ. Eng. 11 (1) (2020) 33–54, https://doi.org/10.1007/s40095-019-00327-y.

[14] Refat Moshery, Chai Tan Yong, Kamaruzzaman Sopian, Fudholi Ahmad, H. Ali, A. Al-Waeli, Thermal performance of jet-impingement solar air heater with transverse ribs absorber plate, Sol. Energy 214 (2021) 355–366, https://doi.org/10.1016/j.solener.2020.11.059. December 2020.

[15] Win Eng Ewe, Ahmad Fudholi, Kamaruzzaman Sopian, Refat Moshery, Nilofar Asim, Wahidin Nuriana, Adnan Ibrahim, Thermo-electro-hydraulic analysis of jet impingement bifacial photovoltaic thermal (JIBPVT) solar air collector, Energy 254 (2022), 124366, https://doi.org/10.1016/j.energy.2022.124366.

[16] Salah M. Salih, Jalal M. Jalil, Saleh E. Najim, Experimental and numerical analysis of double-pass solar air heater utilizing multiple capsules PCM, Renew. Energy 143 (2019) 1053–1066, https://doi.org/10.1016/j.renene.2019.05.050.

[17] Ranchan Chauhan, N.S. Thakur, Tej Singh, Muneesh Sethi, Exergy based modeling and optimization of solar thermal collector provided with impinging air jets, J. King Saud Univ. Eng. Sci. 30 (4) (2018) 355–362, https://doi.org/10.1016/j.jksues.2016.07.003.